Orbital ordering near a Mott transition: Resonant x-ray scattering study of the perovskite Ti oxides $R\mathrm{TiO_3}$ and $\mathrm{LaTiO_{3.02}}$ (R=Gd, Sm, Nd, and La)

M. Kubota*
Photon, Factory, Institute of Materials Structure Science, KEK, Tsukuba 305-0801, Japan

H. Nakao†
Photon, Factory, Institute of Materials Structure Science, KEK, Tsukuba 305-0801, Japan
and Core Research for Evolutional Science and Technology (CREST), Tsukuba 305-0047, Japan

Y. Murakami†
Photon, Factory, Institute of Materials Structure Science, KEK, Tsukuba 305-0801, Japan;
Core Research for Evolutional Science and Technology (CREST), Tsukuba 305-0047, Japan;
and Synchrotron Radiation Research Center, Japan Atomic Energy Research Institute (SPring-8), Mikazuki, Hyogo 679-5148, Japan

Y. Taguchi‡ and M. Iwama
Department of Applied Physics, University of Tokyo, Tokyo 113-8656, Japan

Y. Tokura
Department of Applied Physics, University of Tokyo, Tokyo 113-8656, Japan
and Correlated Electron Research Center (CERC), AIST, Tsukuba 305-0046, Japan
(Received 7 July 2004; published 30 December 2004)

We investigated orbital ordering states in the vicinity of the Mott transition in $R\mathrm{TiO_3}$ and $\mathrm{LaTiO_{3.02}}$ (R=Gd,Sm,Nd,La) using resonant x-ray scattering (RXS) at the $1s\rightarrow 3d$ transition energy of the K absorption edge of Ti. We measured the energy and azimuthal angle dependences of the resonant signal at the reflections of Q=(1 0 0), (0 1 1), and (0 0 1). The RXS intensity gradually decreased with decreasing the $\mathrm{GdFeO_3}$-type distortion. Although there is a magnetic phase boundary between $\mathrm{GdTiO_3}$ (ferromagnet) and $\mathrm{SmTiO_3}$ (antiferromagnet), the ratio among the magnitudes at those reflections was almost the same. The azimuthal angle dependence also showed an identical periodicity at each scattering vector. With further decreasing the $\mathrm{GdFeO_3}$-type distortion, the magnitude of the RXS in $\mathrm{LaTiO_3}$ became small and almost isotropic. This means that the orbital state of $\mathrm{LaTiO_3}$ is different from those of $R\mathrm{TiO_3}$ (R=Y,Gd,Sm). Furthermore, when we approached the Mott transition by hole doping, the signal of the RXS disappeared in $\mathrm{LaTiO_{3.02}}$, which is just located on the metal-insulator boundary. This indicates a disappearance of the orbital ordering at the Mott transition.

DOI: 10.1103/PhysRevB.70.245125 PACS number(s): 71.27.+a, 71.30.+h, 61.10.−i, 71.70.Ej

I. INTRODUCTION

The orbital correlation and the symmetry breaking of orbitals, as well as strong spin and charge correlations, play important roles in rich phase diagrams in strongly correlated electron systems.[1] The importance of the orbital degree of freedom was pointed out in the 1950s concerning the magnetism of $3d$ electron systems.[2] A revival of experimental and theoretical interest in the manganites occurred in the 1990s because of the discovery of colossal magnetoresistance (CMR).[3] In the perovskite-type Mn oxides, Mn^{3+} has a $3d^4$ configuration, in which three electrons occupy the threefold t_{2g} orbitals (xy, yz, and zx) and one electron occupies one of the twofold e_g orbitals (x^2-y^2 and $3z^2-r^2$) owing to strong Hund coupling. Thus, Mn^{3+} has an orbital degree of freedom depending on which e_g orbital is occupied. This orbital degree of freedom can show a long-range order—that is, orbital ordering. Although the experimental technique used to detect the ordering was rather limited, it has recently been found that resonant x-ray scattering (RXS) is a powerful technique to detect orbital ordering through intensive experimental studies.[4–8]

The Ti ion in $R\mathrm{TiO_3}$ (R=Y,Gd,Sm,Nd,La) has one t_{2g} electron, which occupies one of the threefold t_{2g} orbitals. This crystal structure of $R\mathrm{TiO_3}$ is accompanied by a lattice distortion due to a tilting of $\mathrm{TiO_6}$ octahedra ($\mathrm{GdFeO_3}$-type distortion), in which the Ti—O—Ti bond angle along the c axis changes from 140.3° in $\mathrm{YTiO_3}$ to 157.5° in $\mathrm{LaTiO_3}$.[9] By changing R ions, we can control the one-electron bandwidth through the magnitude of the $\mathrm{GdFeO_3}$-type distortion. The magnetic phase diagram is established as a function of the one-electron band width. The ground states of $\mathrm{YTiO_3}$ and $\mathrm{LaTiO_3}$ are a ferromagnetic ($T_C\sim 30$ K) and a G-type antiferromagneitc (AFM) ($T_N\sim 150$ K) insulator, respectively.[10] There is a magnetic phase boundary between $\mathrm{GdTiO_3}$ (ferromagnet) and $\mathrm{SmTiO_3}$ (antiferromagnet) in $R\mathrm{TiO_3}$. Katsufuji *et al.* showed that the $R\mathrm{TiO_3}$ system behaves as a typical Mott insulator through optical conductivity measurements.[10,11] They revealed that the Mott-Hubbard gap (E_g) increases with decreasing ionic radius of R, in propor-

tion with $(U/W)-(U/W)_c$, in which (U/W) is the electron-electron interaction and $(U/W)_c$ corresponds to a hypothetical point for a Mott transition with a half filling. On the other hand, in $LaTiO_{3+\delta/2}$, a small change of the oxygen concentration causes metal-insulator and magnetic transitions. Taguchi *et al.* found that $LaTiO_{3+\delta/2}$ exhibits an antiferromagnetic insulator phase for $\delta<0.05$, an antiferromagnetic metal phase for $\delta=0.06-0.08$, and a paramagnetic metal phase for $\delta>0.08$.[12]

Recently, it has been considered that the orbital degree of freedom takes part in these transport and magnetic properties. For instance, the ferromagnetism in $YTiO_3$ has been theoretically explained by a ferromagnetic superexchange interaction caused by orbital ordering of the t_{2g} electron.[13] Thus, it is significant to study the orbital state in order to understand the transport and magnetic properties. Nakao *et al.* observed the orbital ordering in $YTiO_3$ by using RXS.[14] They determined the pattern of the orbital ordering on Ti sites, which is consistent with the results reproduced by polarized neutron scattering[15] and NMR experiments.[16] On the other hand, in $LaTiO_3$, which shows a smaller $GdFeO_3$-type distortion, Keimer *et al.* detected no RXS signal of the orbital ordering.[17] It is proposed that this is due to the appearance of an orbital liquid state in $LaTiO_3$.[18] By contrast, the importance of the spin-orbit coupling and the Jahn-Teller distortion along the $\langle 111\rangle$ direction also has been pointed out.[19,20] In this way, the changing of the orbital ordering state in $RTiO_3$ has not been clarified, so far. In order to elucidate the changes in the orbital ordering, we intensively performed RXS measurements in $RTiO_3$. A notable point is that we could control the one-electron bandwidth by changing the R ions in $RTiO_3$ without doping, randomness, and structural phase transitions.[21] This is why the insulating $RTiO_3$ compound is an ideal platform to reveal the role of the orbital degree of freedom in the vicinity of the Mott transition.

In the present study, we considered two main topics concerning the orbital ordering of Mott insulators, $RTiO_3$. One was to clarify the relationship between the orbital ordering and the magnetism in this system. The magnetism in the manganites of the e_g electron system, which shows the CMR effect, has a strong correlation with the orbital ordering. On the other hand, the behavior of the orbital ordering in the t_{2g} electron system near a magnetic phase boundary has so far not been investigated in detail. We demonstrated that the orbital state hardly changes between the magnetic phases of a ferromagnet ($GdTiO_3$) and an antiferromagnet ($SmTiO_3$). The other more noteworthy subject is to reveal how the orbital ordering becomes unstable near the Mott transition; the resonant signal corresponding to the orbital ordering continuously decreases with the decrease of the $GdFeO_3$ distortion in the insulating region. Finally, the orbital ordering diminishes completely on the tip of the Mott transition.

The framework of the present paper is as follows. In Sec. II, the experimental procedure and the mechanism of the resonant scatterings at both the pre-edge and the main edge are explained. In Sec. III, we show the experimental results. We remark on the orbital ordering through the magnetic phase boundary in Sec. III A and the suppression of orbital ordering state near the Mott transition in Sec. III B. In Sec. IV, we discuss the relationship between the orbital ordering and the magnetism, in addition to the vanishing process of the orbital ordering. In Sec. V, we summarize the present study.

II. EXPERIMENT

The crystals used in the present study were synthesized by the floating zone technique, as described elsewhere.[10,12] We polished three surfaces corresponding to the scattering planes of $(h\ 0\ 0)$, $(0\ k\ k)$, and $(0\ 0\ l)$. These samples were cut from the same single crystal. X-ray scattering measurements were carried out at beamline X22C at the National Synchrotron Light Source in BNL and at beamline BL-4C, BL-16A2 at the Photon Factory of KEK. The energy resolutions for X22C, BL-4C, and BL-16A2 were about 5 eV, 3 eV, and 1 eV, respectively. Pyrolytic graphite $(0\ 0\ 4)$ reflection was used for the polarization analysis. The incident x-ray beam had σ polarization in the present experimental configuration, while the polarization vector of the x-ray beam within the scattering plane was denoted by π polarization. We measured the azimuthal angle (Ψ) dependence of a resonant energy peak of Ti. Ψ means the rotation angle of a sample around the scattering vector. The origin of Ψ is defined by the configuration in which the polarization of the incident photon beam becomes parallel to the a axis in the case of $(0\ k\ k)$ and to the b axis for both $(h\ 0\ 0)$ and $(0\ 0\ l)$.

We now deal with the mechanism of RXS. Near the K absorption-edge energy, the resonant peaks are observed at the pre-edge and main edge. They correspond to the $1s\rightarrow 3d$ and $1s\rightarrow 4p$ transition energies, respectively. In the present study, the azimuthal angle dependence at the pre-edge was the same as that at the main-edge peak. This result means that the pre-edge peak originates from a dipole transition. In other words, the hybridization between the Ti $4p$ and the neighboring $3d$ orbitally ordered states causes the resonant peak at the pre-edge.[22,23] Therefore, we can recognize the appearance of orbital ordering from the signal at the pre-edge. However, since the signal at the pre-edge contains information concerning the neighboring Ti sites, not that at on sites, it is difficult to analyze the data quantitatively. A theoretical calculation is required for a quantitative analysis of the pre-edge peak. On the other hand, there are two contributions to the origin of the main-edge peak in the RXS, in which we cannot say which mechanism is dominant at the main edge in this stage. One is the interaction between the $4p$ orbital on Ti and the ligand O $2p$ orbital, concomitant with the $GdFeO_3$-type distortion as well as the Jahn-Teller distortion.[22] The $GdFeO_3$-type distortion causes combinations between different t_{2g} orbitals, which is crucial for the (zx^-, yz^+, zx^+, yz^-)-type orbital ordering of $(1/\sqrt{2})(zx-xy)$ (site 1), $(1/\sqrt{2})(yz+xy)$ (site 2), $(1/\sqrt{2})(zx+xy)$ (site 3), and $(1/\sqrt{2})(yz-xy)$ (site 4), in particluar.[13] The other thing is the Coulomb interaction between the $4p$ and $3d$ orbitals due to the orbital ordering.[24] As mentioned later, the pre-edge peak disappears on the border of the Mott transition, while the main-edge peak remains on the Mott transition. In short, the pre-edge peak gives information on the orbital ordering, while the main-edge peak involves the signal from the $GdFeO_3$-type distortion, which is not directly related to the

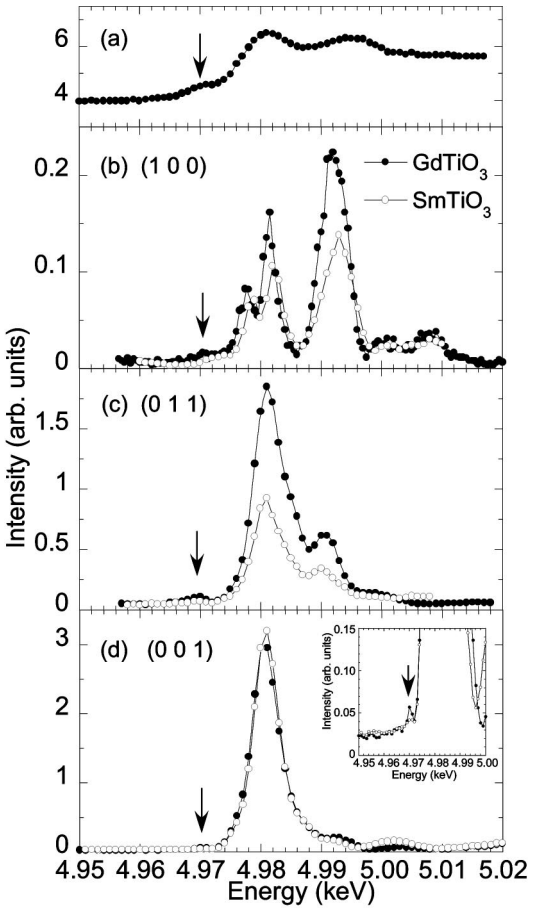

FIG. 1. Energy spectra in $GdTiO_3$ and $SmTiO_3$ by resonant x-ray scattering. (a) X-ray absorption of $GdTiO_3$ measured in the total x-ray fluorescence yield mode. (b)–(d) Energy scans for selected reciprocal positions of (1 0 0) at $\Psi=45°$, (0 1 1) at $\Psi=225°$, and (0 0 1) at $\Psi=0°$. The observed data at $Q=(1\ 0\ 0)$, (0 1 1), and (0 0 1) were normalized by the intensity at $Q=(2\ 0\ 0)$, (0 2 2), and (0 0 2) for each sample, respectively. The arrows indicate the pre-edge peaks.

orbital ordering. Therefore, in this paper, we mainly considered the orbital states based on measurements at the pre-edge.

III. RESULTS

A. Orbital orderings between the magnetic phase boundary

1. Energy profiles

In order to reveal how the orbital ordering changes from that of $YTiO_3$ through the magnetic phase boundary, we performed RXS on $GdTiO_3$ and $SmTiO_3$ at room temperature in the same way with $YTiO_3$.[14]

Figure 1(a) shows the x-ray absorption of $GdTiO_3$ measured in the total x-ray fluorescence yield mode. There is a bump at around 4.971 keV (pre-edge) and a local maximum at around 4.981 keV (main edge), which correspond to the $1s\rightarrow 3d$ and $1s\rightarrow 4p$ dipole transitions, respectively. Next we measured the energy dependence of the RXS intensities at $Q=(1\ 0\ 0)$, (0 1 1), and (0 0 1), around the K absorption edge of the Ti ion in $GdTiO_3$ and $SmTiO_3$. The energy spectra depend on the Q positions, as shown in Figs. 1(b)–1(d) for $GdTiO_3$ (solid circle) and $SmTiO_3$ (open circle). Figure 1(b) shows the energy spectra at $Q=(1\ 0\ 0)$ for $GdTiO_3$ and $SmTiO_3$. The pre-edge peak is observed at 4.971 keV, while the main-edge peaks are seen at 4.978 keV, 4.981 keV, and 4.992 keV. In addition, we observed the pre-edge peaks at $Q=(0\ 1\ 1)$ and $Q=(0\ 0\ 1)$ at 4.970 keV [Figs. 1(c) and 1(d)]. These energy profiles of $GdTiO_3$ and $SmTiO_3$ are similar to those for $YTiO_3$ in Ref. 14.

2. Azimuthal angle dependence

Near to the K absorption edge, the atomic scattering factor (ASF) is represented by a tensor, which reflects an anisotropy of the electron distribution at a selective atomic site. Consequently, the magnitude of the resonant x-ray scattering shows an azimuthal angle (Ψ) dependence. In order to examine the Ψ dependence of the intensity at the pre-edge peak, we performed ω-2θ scans at the pre-edge for each Ψ. The observed data were fitted using a Gaussian profile. The integrated intensities of the resonant peaks for $Q=(1\ 0\ 0)$, (0 1 1), and (0 0 1) were normalized by the integrated intensities at the fundamental positions $Q=(2\ 0\ 0)$, (0 2 2), and (0 0 2), respectively.

Figure 2 shows the Ψ dependence at the pre-edge peaks for $Q=(1\ 0\ 0)$, (0 1 1), and (0 0 1) of $GdTiO_3$ in the left panels [(a)–(d)] and of $SmTiO_3$ in the right panels [(e)–(h)]. The resonant signals at $Q=(1\ 0\ 0)$ [Figs. 2(a) and 2(e)] and (0 0 1) [Figs. 2(d) and 2(h)] with the $I_{\sigma\pi'}$ ($\sigma\rightarrow\pi'$) component[25] have a twofold symmetry for both $GdTiO_3$ and $SmTiO_3$. On the other hand, the signal at $Q=(0\ 1\ 1)$ has both $I_{\sigma\sigma'}$ ($\sigma\rightarrow\sigma'$) [Figs. 2(b) and 2(f)] and $I_{\sigma\pi'}$ [Figs. 2(c) and 2(g)] components. $I_{\sigma\sigma'}$ shows a fourfold symmetry, while $I_{\sigma\pi'}$ shows a 360° period. These results indicate that the orbital orderings have the same symmetry for $GdTiO_3$ and $SmTiO_3$. Besides, we confirmed that the long-range orbital orderings for $GdTiO_3$ and $SmTiO_3$ occur in the direction of the observed Q direction.

Next, we observed the azimuthal angle dependence at the main-edge peak for each scattering vector. Figure 3 shows the Ψ dependence in $GdTiO_3$. The Ψ dependences at the main-edge peak show an identical behavior with those at the pre-edge peak in Figs. 2(a)–2(d) for each scattering vector. This means that the signal at the pre-edge originates from a dipole transition.[22]

B. Suppression of orbital ordered state near the Mott transition

Although the azimuthal angle dependence is identical for each Q, and the energy spectra are analogous among $R\mathrm{TiO_3}$ (R=Y, Gd, Sm), the magnitude of the resonant signal in $SmTiO_3$ is smaller than that in $GdTiO_3$, as shown in Fig. 2. Thus, in order to clarify the orbital ordered state near the Mott transition, we performed the RXS of $R\mathrm{TiO_3}$ (R=Nd, La).

The magnitude of the resonant signal in $NdTiO_3$ becomes weaker than that in $SmTiO_3$. It is well known that $LaTiO_3$

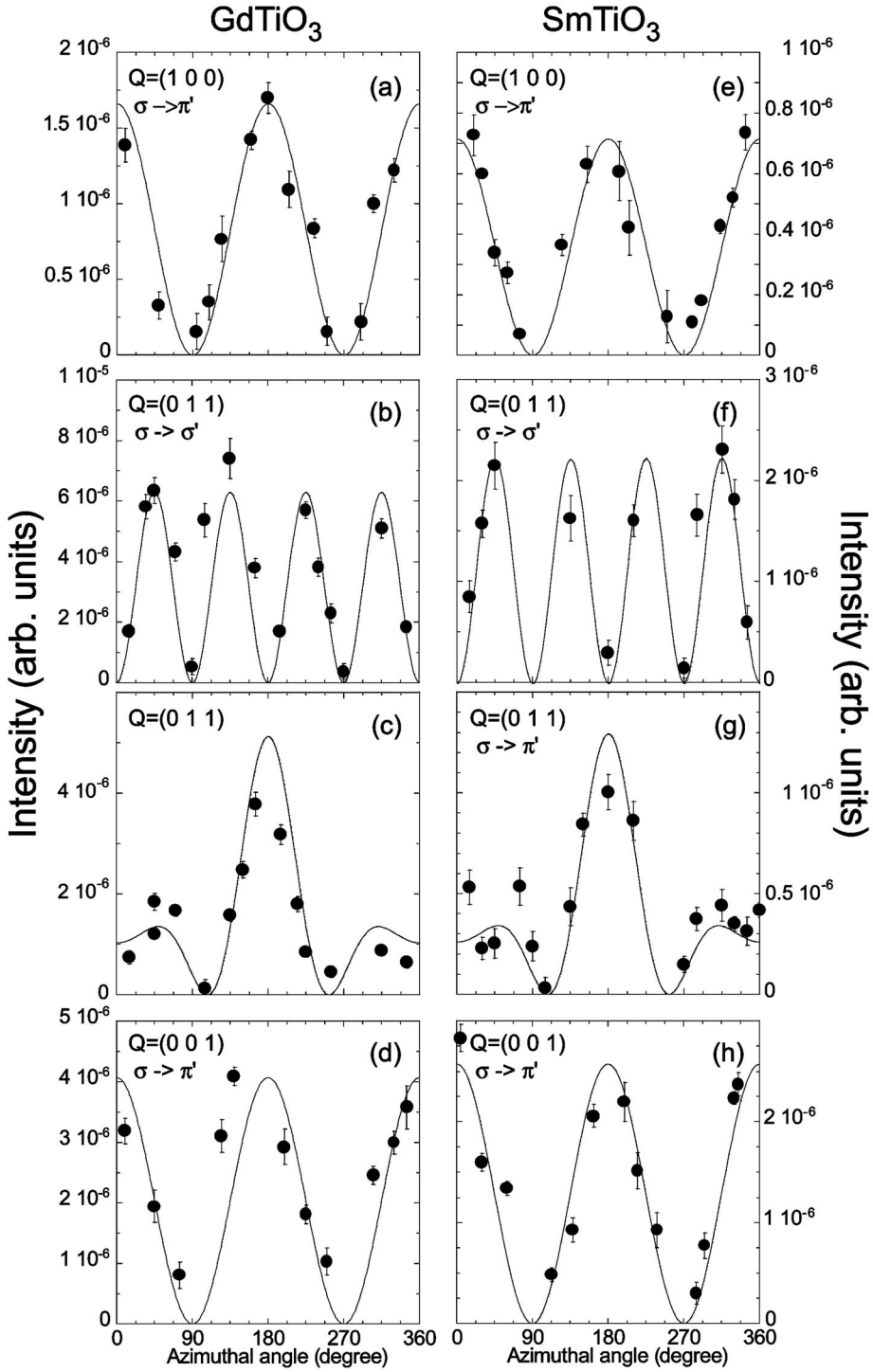

FIG. 2. Azimuthal angle dependences of the magnitude at the pre-edge peaks for $Q=(1\ 0\ 0)$, $(0\ 1\ 1)$, and $(0\ 0\ 1)$ in $GdTiO_3$ (left panels) and $SmTiO_3$ (right panels). For $Q=(0\ 1\ 1)$, the dependences are shown in the process of both $\sigma \rightarrow \sigma'$ and both $\sigma \rightarrow \pi'$. The origin of Ψ is the condition in which the polarization of the incident photon beam becomes parallel to the a axis in the case of $(h\ 0\ 0)$ and to the b axis for $(0\ 0\ l)$. The lines are guides to the eye.

shows an AFM insulating behavior ($T_N \sim 150$ K) with a small optical gap of 0.1 eV.[26] The energy profiles were measured at $Q=(1\ 0\ 0)$ and $(0\ 0\ 1)$ with the $\Psi=0°$, in which the pre-edge appeared at 4.971 keV. We successfully observed the resonant signal in $LaTiO_3$.[27] The energy profiles are similar to those in other $R TiO_3$ compounds in terms of the profile shapes and the energy peak positions (Fig. 4). The azimuthal angle dependence at the main-edge peak has the same character of twofold symmetry at $Q=(1\ 0\ 0)$ and $(0\ 0\ 1)$, as shown in Fig. 5. Considering that $LaTiO_3$ is accompanied by a finite tilting angle of TiO_3 octahedra of 157.6°, these results indicate that the main-edge peaks in $R TiO_3$ mainly originate from a $GdFeO_3$-type distortion.

We furthermore measured the compound $LaTiO_{3.02}$, which shows an AFM insulating behavior ($T_N \sim 125$ K). $LaTiO_{3.02}$ is located near the Mott transition phase boundary between an AFM insulator and an AFM metal.[12] We performed an energy scan at $Q=(0\ 0\ 1)$, and the signal at the main edge was obtained, in which the energy spectra above 4.981 keV had almost the same structure as that in $LaTiO_3$. However, no signal at the pre-edge was observed, as shown in the inset of Fig. 4, in contrast with the signal in $LaTiO_3$.

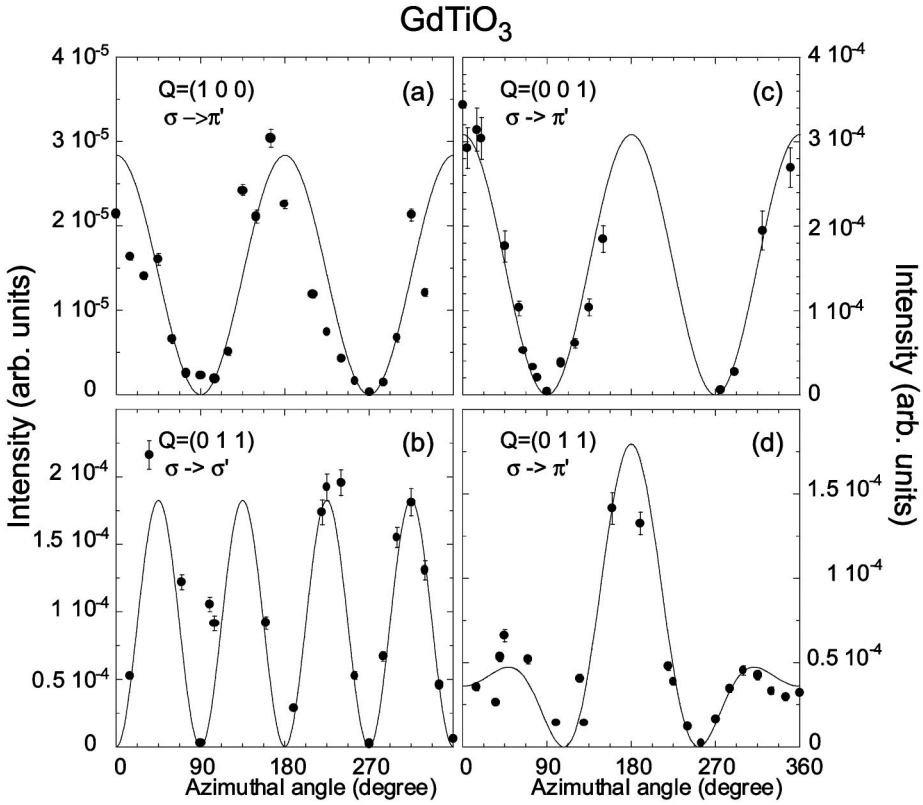

FIG. 3. Azimuthal angle dependences of the magnitude at the main-edge peaks for $Q=(1\ 0\ 0)$ (a), (0 1 1) (b), (d), and (0 0 1) (c) in $GdTiO_3$. The observed data at $Q=(1\ 0\ 0)$, (0 1 1) and (0 0 1) are normalized by the intensity at $Q=(2\ 0\ 0)$, (0 2 2), and (0 0 2), respectively. The solid line curves indicate analysis results.

This indicates that a complete suppression of the orbital ordering was observed in $LaTiO_{3.02}$.

IV. DISCUSSION

Let us discuss the vanishing process of the orbital ordering in RTiO$_3$. For a comparison, the intensity of the pre-edge signal was normalized by an observed fundamental peak and was furthermore corrected considering the ratio of a structure factor at a fundamental position in RTiO$_3$ to that at $Q=(2\ 0\ 0)$ in $YTiO_3$.[9] In Fig. 6, the corrected magnitude of the pre-edge peak is plotted as a function of the Ti—O—Ti bond angle along the c axis (the lower horizontal axis) and the one-electron bandwidth W (the upper horizontal axis), which is cited in Ref. 10.

A. Orbital orderings through the magnetic phase transition

While a vanishing of the orbital ordering occurs, RTiO$_3$ varies from ferromagnet ($GdTiO_3$) to antiferromagnet ($SmTiO_3$). We first compared the pre-edge peaks for $GdTiO_3$ and $SmTiO_3$. For the pre-edge peaks, the ratio among the magnitudes at $Q=(1\ 0\ 0)$, (0 1 1), and (0 0 1) was about 2:3:4 in common with both compounds, although the absolute magnitudes in $GdTiO_3$ were larger than that in $SmTiO_3$, as shown Fig. 6. Next, we examined the intensity of the main-edge peaks for both compounds, since the significance of the $GdFeO_3$-type distortion has been pointed out theoretically concerning the orbital ordering of $YTiO_3$: Mizokawa and Fujimori revealed that due to a large $GdFeO_3$-type distortion, the covalency between the R site cationsand oxygen ions makes the d-type Jahn-Teller distortion stabilized.[28] In addition, Mochizuki and Fujimori insisted that a large $GdFeO_3$-type distortion causes the strong stability of the (zx^-,yz^+,zx^+,yz^-)-type orbital ordering, as observed in $YTiO_3$.[20] From this point of view, it is likely that the main edge accompanied with the $GdFeO_3$-type distortion shows indirect information on the degree of the stabilization, as for the (zx^-,yz^+,zx^+,yz^-)-type orbital ordering. A comparison of the resonant signals at the pre-edge and main edge in $GdTiO_3$ and $SmTiO_3$ indicates that a slight change of the anisotropy of electron distribution at a Ti site occurs with the same local symmetry, in which $zx(yz)$ combines with xy at every site with a ratio of 1:1 approximately for both $GdTiO_3$ and $SmTiO_3$, similar to the orbital ordering in $YTiO_3$.

Mochizuki and Imada argue that under the unchanging of the orbital ordering in FM phase and AFM phases, the A-type AFM structure should appear in the vicinity of the magnetic phase boundary.[20] The A-type AFM structure has ferromagnetic planes, stacked with an AFM coupling along c. Amow *et al.* observed the magnetic signal of the G-type AFM structure on Ti sites, concomitant with that of the C-type AFM structure on Sm sites in $Sm_{0.97}TiO_3$ by neutron diffraction measurements.[29,30] Thus, in $SmTiO_3$, the induced field generated by the magnetic rare-earth ion has the possibility to influence the Ti site. Since the theoretical work by Mochizuki and Imada does not consider the induced field, the significance of the A-type AFM instability remains an open problem in the vicinity of the magnetic phase boundary of RTiO$_3$. However, we can definitely conclude that the local symmetry at a Ti site hardly changes between $GdTiO_3$ and $SmTiO_3$.

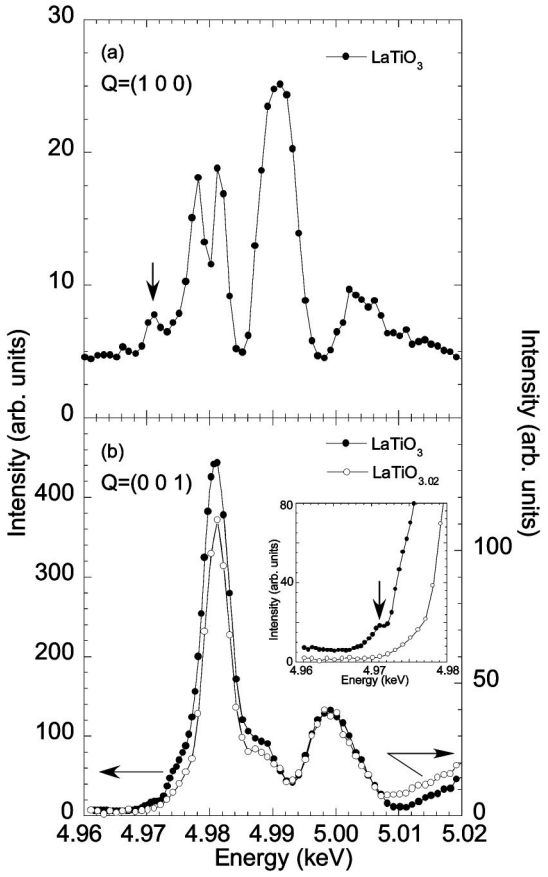

FIG. 4. (a) Energy profile at $Q=(1\ 0\ 0)$ in $LaTiO_3$ at $\Psi=0°$. The pre-edge peak is observed. (b) Energy profiles at $Q=(0\ 0\ 1)$ in both $LaTiO_3$ and $LaTiO_{3.02}$ with $\Psi=0°$. The main-edge peaks are detected for the two compounds. However, the pre-edge peak appears in only $LaTiO_3$, as shown in the inset.

B. Vanishing process of orbital ordering near the Mott transition

The pre-edge peak continuously diminishes with an increase of the tilting angle and the one-electron bandwidth in Fig. 6. This consecutive change is consistent with the prediction by Mochizuki and Imada.[31] The magnitude seems to reach zero at the Mott transition with a critical bandwidth

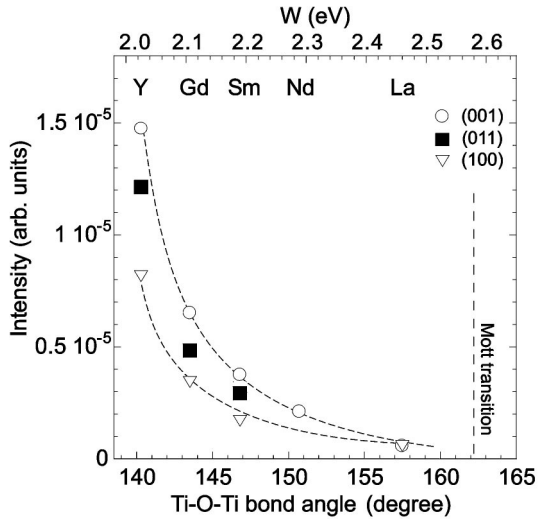

FIG. 6. Magnitude of the pre-edge peaks at $Q=(1\ 0\ 0)$, $(0\ 1\ 1)$, and $(0\ 0\ 1)$ as a function of the Ti—O—Ti bond angle along the c axis (the lower horizontal axis) and the one-electron bandwidth W (the upper horizontal axis). The one-electron band width is cited in Ref. 10. The pre-edge peak vanishes on the tip of Mott transition. All data were normalized by an observed fundamental peak and were furthermore corrected, considering the ratio of a structure factor at a fundamental position in $RTiO_3$ to that at $Q=(2\ 0\ 0)$ in $YTiO_3$.

(W_c) of $\sim$2.58 eV.[32] This behavior is in strong contrast with the changes in the magnitude of the main-edge peak, in which a finite magnitude remains near the Mott transition, as is seen in the spectrum of $LaTiO_{3.02}$ in Fig. 4. The ratio of the intensities at the pre-edge among $Q=(1\ 0\ 0)$, $(0\ 1\ 1)$, and $(0\ 0\ 1)$ is different between for a large and a small tilting of the TiO_6 octahedron in Fig. 6. As for $RTiO_3$ (R=Y, Gd, and Sm), the magnitude at $Q=(1\ 0\ 0)$ is about half as large as that at $Q=(0\ 0\ 1)$, while the magnitudes at the pre-edge peak for $LaTiO_3$ are almost the same at both $Q=(1\ 0\ 0)$ and $(0\ 0\ 1)$. In contrast with the same Ψ dependence, the Q dependence of the magnitude for the pre-edge peak in $LaTiO_3$ is totally different from that in $RTiO_3$ (R=Y, Gd, Sm). This means that the orbital ordered state in $LaTiO_3$ varies from those in $RTiO_3$ (R=Y, Gd, Sm). Considering these results, one can safely state that the magnitude of the tilting of the TiO_6 octahedron in $LaTiO_3$ is not sufficient to stabilize the

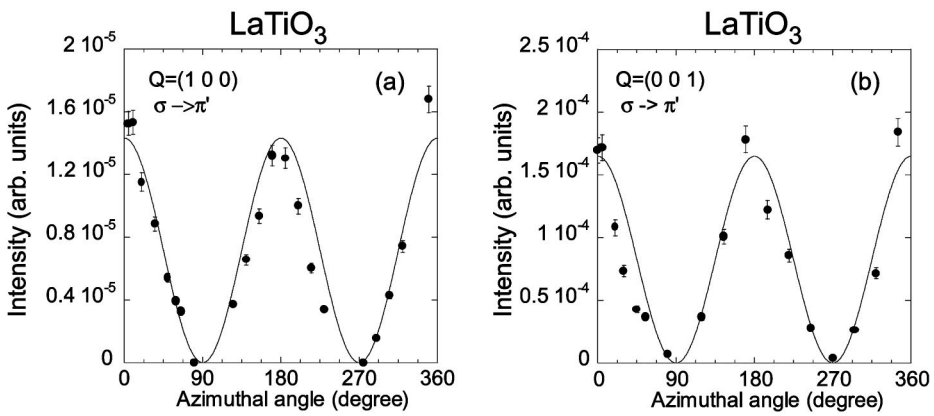

FIG. 5. Azimuthal angle dependences of the magnitude at the main-edge peaks for (a) $Q=(1\ 0\ 0)$ and (b) $(0\ 0\ 1)$ in $LaTiO_3$. All of the observed data are normalized by the intensity at a fundamental position. The solid line curves indicate the analysis results.

(zx^-, yz^+, zx^+, yz^-)-type orbital ordering due to the superexchange interaction accompanied by the covalency between the *R* ion and the oxygen ion, which is consistent with a prediction by Mizokawa and Imada.[20] and/or by Mochizuki and Fujimori[28]

The full width at half maximum (FWHM) in the pre-edge profile of $LaTiO_3$ corresponds to the equipment resolution limit for the space and energy regions, which means that the orbital ordering shows a long-range order. On the other hand, the orbital ordering disappears, owing to only a subtle mobility of carriers in $LaTiO_{3.02}$, which is located on the tip of Mott transition.[12] This means that the orbital ordering is robust, accompanied by a long-range correlation, even in the vicinity of the Mott transition. To sum up, it has been revealed that the degeneracy of three t_{2g} orbital levels is lifted in the AFM insulator phase, and then the Mott transition occurs with the degeneracy of the t_{2g} orbitals in the AFM metal phase. It seems that the orbital ordering in $R\mathrm{TiO}_3$ stabilizes the insulating behavior near the Mott transition.

V. CONCLUDING REMARKS

We intensively investigated the orbital-ordered state in the Mott insulator $R\mathrm{TiO}_3$ (R=Gd, Sm, Nd, La) and $LaTiO_3$ compounds using the resonant x-ray scattering technique. We established the behavior of the orbital ordering near the Mott transition. For the range with a large $GdFeO_3$-type distortion, the (zx^-, yz^+, zx^+, yz^-)-type orbital ordering is stabilized. This distortion causes the covalency between the *R*-site cation and oxygen ions, which reproduces the combination of different t_{2g} orbitals. With lowering the $GdFeO_3$-type distortion, the resonant signal from the orbital ordering gradually decreases, accompanied by the same local symmetry between $GdTiO_3$ (ferromagnet) and $SmTiO_3$ (antiferromagnet). For a small $GdFeO_3$-type distortion, the above orbital ordering pattern changes in $LaTiO_3$. Below the threshold of the $GdFeO_3$-type distortion, the orbital ordering becomes unstable. We have found that the orbital ordering disappears in $LaTiO_{3.02}$, which is located on the boundary between the AFM insulating phase and the AFM metallic phase.

ACKNOWLEDGMENTS

The present work was performed at the NSLS (BNL), which is supported by the U.S. DOE, Division of Materials Science and Division of Chemical Science (Contact No. DE-AC02-98CH10886) and has been carried out under the approval of the Photon Factory Program Advisory Committee (Proposal No. 2001S2-002). This study was supported by Core Research for Evolutional Science and Technology (CREST).

*Electronic address: masato.kubota@kek.jp
†Present address: Department of Physics, Tohoku University, Aoba-ku, Sendai 980-8578, Japan.
‡Present address: Institute for Materials Research, Tohoku University, Aoba-ku, Sendai 980-8577, Japan.

[1] M. Imada, A. Fujimori, and Y. Tokura, Rev. Mod. Phys. **70**, 1039 (1998).
[2] C. Zener, Phys. Rev. **82**, 403 (1951); P. W. Anderson and H. Hasegawa, *ibid.* **100**, 675 (1955); P. G. de Gennes, Phys. Rev. **118**, 141 (1960).
[3] Y. Tokura, A. Urushibara, Y. Moritomo, T. Arima, A. Asamitsu, G. Kido, and N. Furukawa, J. Phys. Soc. Jpn. **63**, 3931(1994); P. Schiffer, A. P. Ramirez, W. Bao, and S.-W. Cheong, Phys. Rev. Lett. **75**, 3336 (1995); Y. Tokura, Y. Tomioka, H. Kuwahara, A. Asamitsu, Y. Moritomo, and M. Kasai, J. Appl. Phys. **79**, 5288 (1996).
[4] Y. Murakami, H. Kawada, H. Kawata, M. Tanaka, T. Arima, Y. Moritomo, and Y. Tokura, Phys. Rev. Lett. **80**, 1932 (1998).
[5] Y. Murakami, J. P. Hill, D. Gibbs, M. Blume, I. Koyama, M. Tanaka, H. Kawata, T. Arima, Y. Tokura, K. Hirota, and Y. Endoh, Phys. Rev. Lett. **81**, 582 (1998).
[6] Y. Endoh, K. Hirota, S. Ishihara, S. Okamoto, Y. Murakami, A. Nishizawa, T. Fukuda, H. Kimura, H. Nojiri, K. Kaneko, and S. Maekawa, Phys. Rev. Lett. **82**, 4328 (1999).
[7] K. Nakamura, T. Arima, A. Nakazawa, Y. Wakabayashi, and Y. Murakami, Phys. Rev. B **60**, 2425 (1999).
[8] M. V. Zimmermann, J. P. Hill, D. Gibbs, M. Blume, D. Casa, B. Keimer, Y. Murakami, Y. Tomioka, and Y. Tokura, Phys. Rev. Lett. **83**, 4872 (1999).
[9] D. A. Maclean, H.-N. Ng, and J. E. Greedan, J. Solid State Chem. **30**, 35 (1979); C. W. Turner and J. E. Greedan, *ibid.* **34**, 207 (1980).
[10] T. Katsufuji, Y. Taguchi, and Y. Tokura, Phys. Rev. B **56**, 10145 (1997).
[11] T. Katsufuji, Y. Okimoto, and Y. Tokura, Phys. Rev. Lett. **75**, 3497 (1995).
[12] Y. Taguchi, T. Okuda, M. Ohashi, C. Murayama, N. Mori, Y. Iye, and Y. Tokura, Phys. Rev. B **59**, 7917 (1999).
[13] T. Mizokawa, D. I. Khomskii, and G. A. Sawatzky, Phys. Rev. B **60**, 7309 (1999).
[14] H. Nakao, Y. Wakabayashi, T. Kiyama, Y. Murakami, M. v. Zimmermann, J. P. Hill, D. Gibbs, S. Ishihara, Y. Taguchi, and Y. Tokura, Phys. Rev. B **66**, 184419 (2002).
[15] H. Ichikawa, J. Akimitsu, M. Nishi, and K. Kakurai, Physica B **281&282**, 482 (2000); J. Akimitsu, H. Ichikawa, N. Eguchi, T. Miyano, M. Nishi, and K. Kakurai, J. Phys. Soc. Jpn. **70**, 3475 (2001).
[16] M. Itoh, M. Tsuchiya, H. Tanaka, and K. Motoya, J. Phys. Soc. Jpn. **68**, 2783 (1999).
[17] B. Keimer, D. Casa, A. Ivanov, J. W. Lynn, M. v. Zimmermann, J. P. Hill, D. Gibbs, Y. Taguchi, and Y. Tokura, Phys. Rev. Lett. **85**, 3946 (2000).
[18] G. Khalliullin and S. Maekawa, Phys. Rev. Lett. **85**, 3950 (2000).
[19] T. Jo, J. Phys. Soc. Jpn. **70**, 3180 (2001).
[20] M. Mochizuki and M. Imada, J. Phys. Soc. Jpn. **69**, 1982 (2000); **70**, 1777 (2001).
[21] As for the doped Ti oxides such as $La_{1-x}Sr_xTiO_3$ and $Y_{1-x}Ca_xTiO_3$, mobile carrier has a tendency of disturbing the

orbital ordering. Therefore we need to consider the change of both the band filling and the electron-electron correlation by the substitution of Sr(Ca) for La(Y) ion.

[22] M. Takahashi and J. Igarashi, Phys. Rev. B **64**, 075110 (2001).

[23] M. Takahashi, J. Igarashi, and P. Flude, J. Phys. Soc. Jpn. **69**, 1614 (2000).

[24] S. Ishihara, T. Hatakeyama, and S. Maekawa, Phys. Rev. B **65**, 064442 (2002).

[25] $I_{\sigma\sigma'}$ ($I_{\sigma\pi'}$) means the resonant signal, (un)accompanied by a change of the polarization direction of the x-ray beam after scattering.

[26] Y. Okimoto, T. Katsufuji, Y. Okada, T. Arima, and Y. Tokura, Phys. Rev. B **51**, 9581 (1995).

[27] We comment on the orbital-ordered state in $LaTiO_3$. The $GdFeO_3$-type distortion mainly contributes to the appearing of the main-edge peak, while the pre-edge peak reflects on the orbital ordering. Consequently the main-edge peak should be observed even at the Mott transition due to the $GdFeO_3$-type distortion, although the pre-edge peak vanishes. Keimer *et al.* detected no resonant signal for both the pre-edge and main-edge peaks in $LaTiO_3$ (Ref. 17). The discrepancy between their results and the present results is just due to the difference of the ratio of the signal to the noise level (S/N) in the observation.

[28] T. Mizokawa and A. Fujimori, Phys. Rev. B **54**, 5368 (1996).

[29] G. Amow, J. E. Greedan, and C. Ritter, J. Solid State Chem. **141**, 262 (1998).

[30] In the *G*-type AFM structure, spin moments between the nearest sites have AFM couplings for every direction, while in the *C*-type AFM structure, ferromagnetic chains along the *c* axis couple antiferromagnetically.

[31] M. Mochizuki and M. Imada, cond-mat/0403031 (unpublished).

[32] The critical bandwidth W_c at the Mott transition is reproduced, considering that the Mott transition occurs with a finite value $\widetilde{W}^{-1}(\sim 0.95)$ and the bandwidth of $LaTiO_3$ is 2.45 eV, in Ref. 10.